Astrophys. Space Sci. Trans., 7, 21–27, 2011
www.astrophys-space-sci-trans.net/7/21/2011/
doi:10.5194/astra-7-21-2011

ASTRA
Astrophysics and Space Sciences Transactions

Simulation of Charged Particle Diffusion in MHD plasmas

F. Spanier and M. Wisniewski

Lehrstuhl für Astronomie, Universität Würzburg, Germany

Received: 18 September 2010 – Revised: 20 December 2010 – Accepted: 20 December 2010 – Published: 19 January 2011

Abstract. Magnetohydrodynamical simulations of turbulent plasmas have been performed to study the transport of energetic test particles. Several parameters of the underlying MHD simulation have been varied to gain insight into the main processes governing transport. Here also the distinct effects of wave-particle resonance and field line wandering shall be studied.

1 Introduction

The transport of energetic particles in turbulent magnetic fields has been studied in last decades by means of analytical theory. Quasilinear theory (Jokipii, 1966; Schlickeiser, 1989) has explained many details of the transport phenomenology, but is limited by simplifying assumptions about the underlying turbulence. Extensions like the nonlinear guiding center theory Shalchi et al. (2004) have been used to understand the perpendicular diffusions coefficient. Second-order quasilinear theory (Shalchi, 2005; Tautz et al., 2008) has also been applied to understand the behaviour of charged particle diffusion beyond the quasilinear theory.

Simulations on the other hand are not limited by simplifications to ease calculations, but also here the turbulence used for the particle transport is usually only implemented through statistical fluctuations (see Qin et al., 2006). This results in an incomplete representation of real turbulence encountered in the interstellar medium and the heliosphere.

We will present our approach to the simulation of the transport parameters: using compressible as well as incompressible MHD, simulations have been performed providing turbulent fields consistent with MHD theory. This approach may be used for interstellar plasma (Armstrong et al., 1995) or the heliosphere (Balogh et al., 1995), but in both cases we have to limit the numerical resolution, since realistic turbulent spectra range over 3–10 orders of magnitude. Employing a test-particle approach energetic particle trajectories are simulated. From these trajectories the Fokker-Planck-coefficients may then be computed. A major advantage of this approach is the possibility of using realistic turbulent spectra, which are anisotropic in the presence of background magnetic fields (Goldreich and Sridhar, 1995), to determine transport parameters.

The results presented include the pitch-angle diffusion coefficient $D_{\mu\mu}$ and the momentum diffusion coefficient D_{pp} for incompressible and compressible plasma. We will identify the physical processes contributing to scattering and analyse the relative importance. Specific applications and resulting observable quantities as the mean free path will be published in a forthcoming paper.

2 Numerical method

For the evolution of the background magnetic fields the ideal, isothermal MHD equations have been solved:

$$\frac{\partial \rho}{\partial t} = -\nabla \boldsymbol{s} \tag{1}$$

$$\frac{\partial \boldsymbol{s}}{\partial t} = -\nabla \left(\frac{\boldsymbol{s}\boldsymbol{s}}{\rho} + \left(p + \frac{B^2}{2} \right) 1 - \boldsymbol{B}\boldsymbol{B} \right) + \boldsymbol{F} \tag{2}$$

$$\frac{\partial \boldsymbol{B}}{\partial t} = -\nabla \left(\frac{\boldsymbol{s}\boldsymbol{B} - \boldsymbol{B}\boldsymbol{s}}{\rho} \right) \tag{3}$$

$$p = \frac{c_s^2}{u_0^2} \rho \overset{(here)}{=} \rho \tag{4}$$

where s is the momentum density $\rho \boldsymbol{v}$. The CWENO method (Kurganov and Petrova, 2001) has been used to solve this hyperbolic problem using the implementation from Kissmann

Correspondence to: F. Spanier
(fspanier@astro.uni-wuerzburg.de)

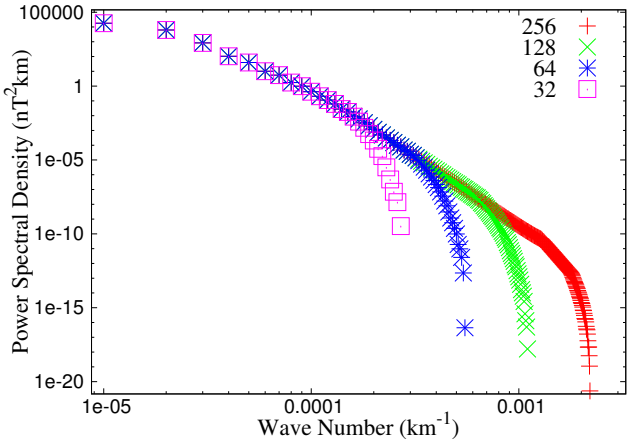

Fig. 1. Simulated spectra for different grid sizes

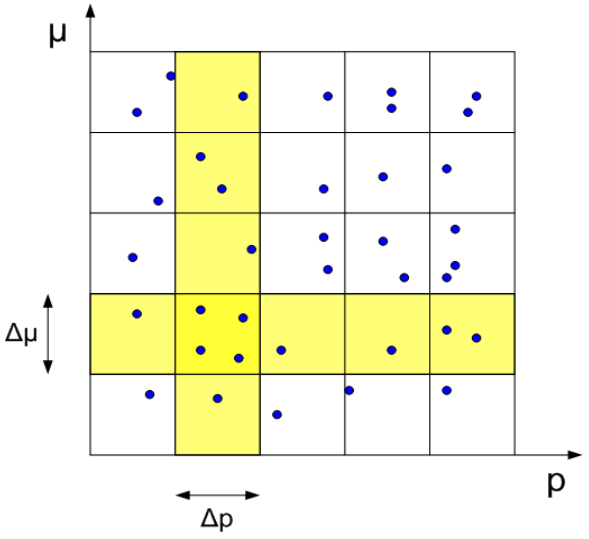

Fig. 2. Division of the parameter space for the particles in the pitch-angle momentum phasespace

and Grauer (2007). The force $\boldsymbol{F}$ describes the external forcing of the plasma, we will specify it below.

In this compressible MHD ansatz two different drivers have been used: On large scales energy has been injected into the velocity field either as compressible ($\nabla \times \boldsymbol{v}=0$) or incompressible ($\nabla \cdot \boldsymbol{v}=0$) velocity. This corresponds to different physical mechanism of driving: Shocks (de Avillez and Breitschwerdt, 2007) or streaming particles (Riquelme and Spitkovsky, 2009). Simulations have been carried out in high- and low- plasma-β environments. The simulations have been carried out on different grid sizes (Fig. 1) to show the effect of the grid size on the transport parameters. Finally a 64^3 grid with periodic boundary conditions has been used.

With the fluid fields given by the MHD equations the

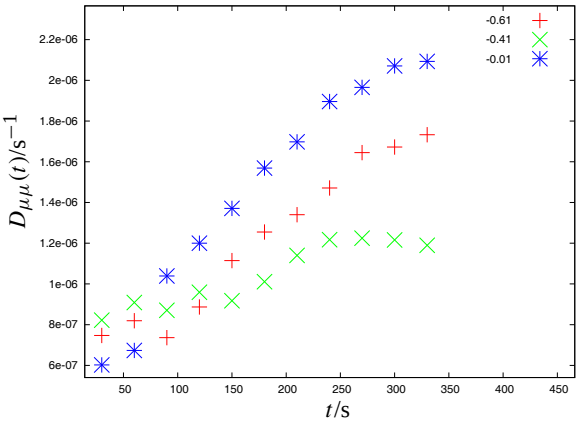

Fig. 3. Temporal evolution of the running diffusion coefficient $D_{\mu\mu}$ for different propagation angles. It can be seen that the values converge. Shown are curves for different initial pitch angles.

Lorentz force on the particles is calculated by

$$\boldsymbol{F}_p = q(\boldsymbol{E} + \boldsymbol{v} \times \boldsymbol{B})$$
$$\boldsymbol{E} = -\boldsymbol{u} \times \boldsymbol{B}$$

using the ideal Ohm's law. While this is physically correct it still gives a much too coarse gridding of the forces. Here cubic splines are used to interpolate the fields. Preliminary studies have shown that linear spline are not enhancing the numerical accuracy.

The transport parameters are then derived by following the particles' paths and calculating

$$D_{\mu\mu} = \lim_{t\to\infty} \frac{1}{2} \frac{\langle(\Delta\mu)^2\rangle}{t}$$
$$D_{pp} = \lim_{t\to\infty} \frac{1}{2} \frac{\langle(\Delta p)^2\rangle}{t}$$

which are assigned to initial μ, p (Fig. 2). In the derivation of the transport parameters no assumptions about turbulence geometry or wave-particle interactions have been made. It has been argued (Fichtner, 2010) that this definition of especially the pitch-angle coefficient may be ill-defined due to the finite value range of μ. To validate our results we closely monitored the temporal evolution of the running diffusion coefficients (Fig. 3). Here the increase of the diffusion coefficient and its convergent value can be seen. A decrease due to the finiteness of μ is not seen. Details of the convergence can be seen in the final result plots.

3 Physical processes

To understand the interaction of energetic particles with the turbulence, we are trying to divide the interaction into different subprocesses. The first cases should prove that the code is working physically correct, while the extended test cases shall give more insight into the actual diffusion process.

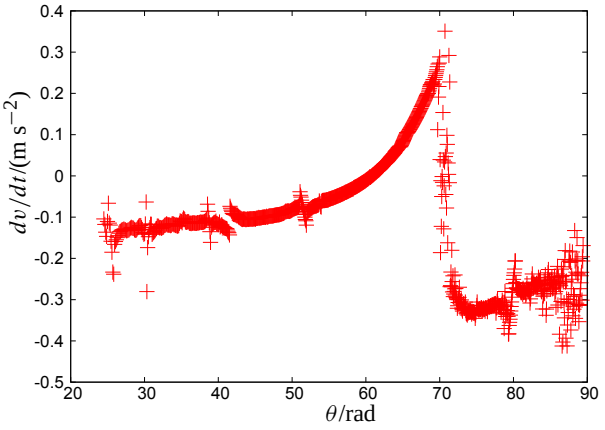

Fig. 4. Acceleration of particles in wave-particle-interaction. In this setup we expect a gyroresonance at 70° and 79°. This can be clearly detected here.

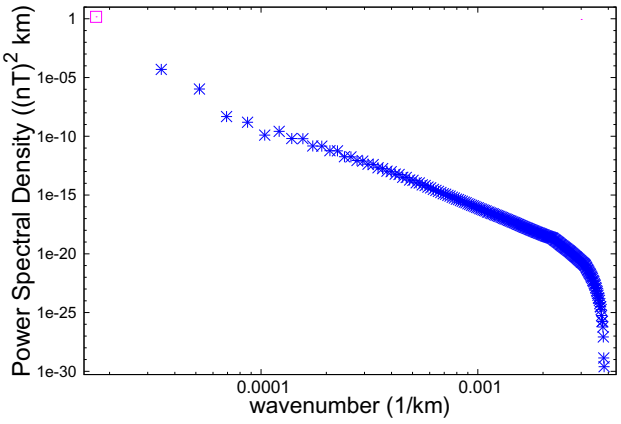

Fig. 5. Spectrum for driving with $k=1$, squares denote the driving spectrum, stars undriven modes

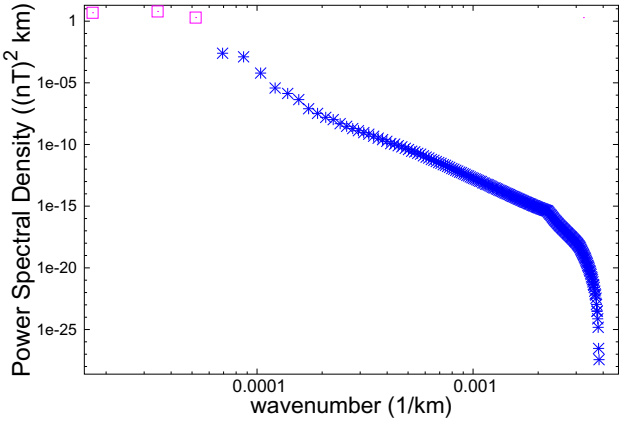

Fig. 6. Spectrum for driving with $k=1$ and $k=2$, squares denote the driving spectrum, stars undriven modes

3.1 Analytical test case

The most simple test cases which have been conducted are the convection and gyration of energetic particles in uniform magnetic field or in the absence of magnetic fields. This has been performed to check the limit of stability and it could be shown that with the given algorithm the analytical behaviour could be reproduced.

For all test cases a box size of 10^{17} cm has been used. This is motivated by length scales inferred from the interstellar medium. The box is cubic not preferring 2D or slab-like turbulence. We refrained from using box anisotropies as used in Maron and Goldreich (2001), since those might affect the transport parameters strongly.

3.2 Gyroresonance test case

A more sophisticated test case is the interaction of an energetic particle with one single wave. While there is no full analytical solution for this problem, we can still look for resonances in the change of momentum. In Fig. 4 one Alfvén wave has been assumed and a population of energetic particles with identical momentum and isotropic distribution with respect to the background magnetic field. Using the resonance condition

$$k_\parallel v\mu - \omega = n\Omega_i \quad n = \ldots -1, 0, 1, \ldots \tag{5}$$

In the specific test case one expects that gyroresonances would be expected for the particle propagation angles 70° and 79°, which is clearly detected. So the code is able to cope this important test case.

3.3 Fundamental wave test case

For the first test case energy (with compressible or incompressible modes) has been injected only on the largest scale ($k=1$, which can be represented as a delta-function for the external force $\boldsymbol{F}$ in Fourier space) and has been evolving. The spectrum can be seen in Fig. 5. Energetic particles are put into the simulation isotropically and uniformly. The test case has been performed with two different super-Alfvénic, subrelativistic particle species (10^5 and $7\cdot10^5\,\mathrm{m\,s^{-1}}$).

3.4 Higher order wave test case

For the second test case energy has been injected on the two largest scales ($k=1$ and 2) and has been evolving. The spectrum can be seen in Fig. 6. The rest of the setup is similar to the first test case.

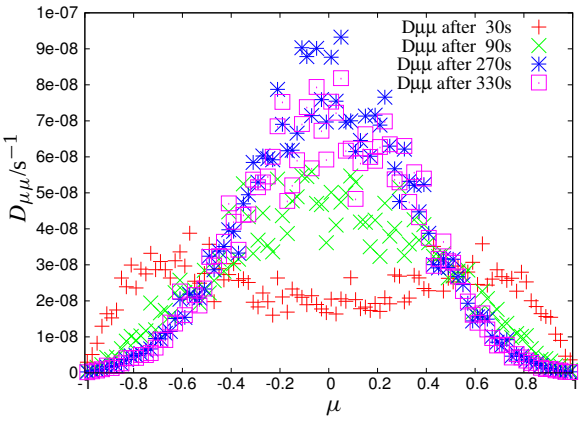

Fig. 7. Pitch angle diffusion coefficient for slow particles, compressible driving, driving $k = 1$ and 2

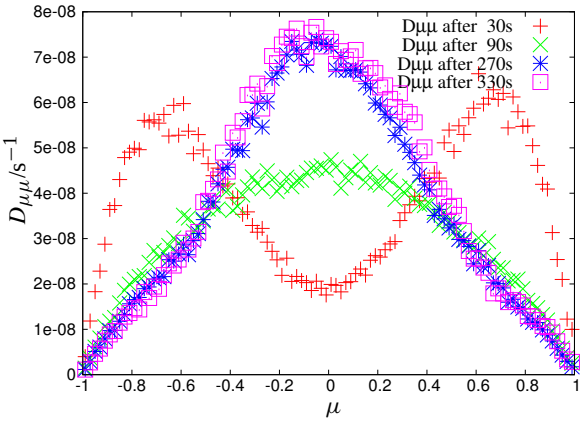

Fig. 9. Pitch angle diffusion coefficient for slow particles, incompressible driving, driving $k = 1$ and 2

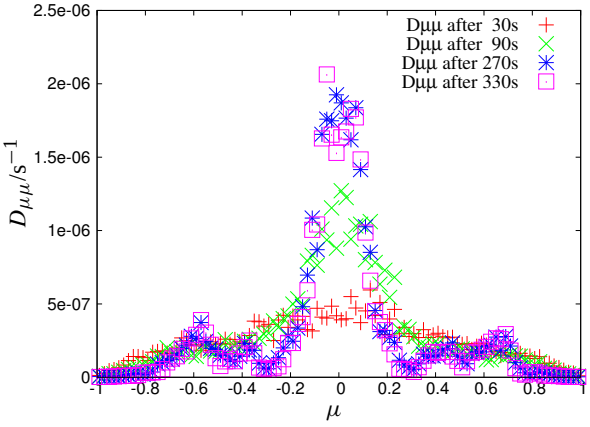

Fig. 8. Pitch angle diffusion coefficient for fast particles, compressible driving, driving $k = 1$ and 2

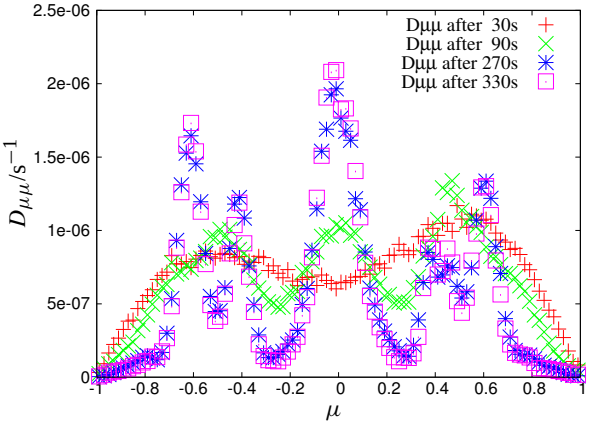

Fig. 10. Pitch angle diffusion coefficient for fast particles, incompressible driving, driving $k = 1$ and 2

4 Results

4.1 Comparison of compressible and incompressible driving

For the higher order wave test case we have performed simulations for both drivers (compressible and incompressible) and both particle speeds. The resulting pitch angle diffusion coefficients are shown in Figs. 7 – 10.

One obvious result is, that for the case of slow particles the pitch angle diffusion coefficient evolves from a more or less clear double hump structure (which represents the QLT result for resonant scattering, but might be also a feature of the gyration itself) to a strong scattering through $\mu = 0$. For fast particles the initial running diffusion coefficients look similar, but evolve to a structure in which the gyroresonances of the particles can be identified. Also for the fast particles a clear difference between compressible and incompressible driving is visible. While in both cases the amplitude of the $\mu = 0$ scattering is similar, the scattering through the gyroresonances is strongly suppressed for compressible driving. This suggests that the resonances are essentially with fast magnetosonic modes and Alfvén modes which are not strongly excited in the compressible case. Additionally the width of the scattering through $\mu = 0$ between slow and fast particles may be explained by present wave damping, which should be stronger for slow particles (Shalchi et al., 2008).

4.2 Comparison of driving range width

We also compared the effect of changing the driving range from the higher order to the fundamental wave test case. Here only incompressible modes have been used. The slow particle test case is shown in Fig. 11 (to be compared with Fig. 9). Fast particles are shown in Fig. 12 (to be compared with Fig. 10).

For the slow particles the differences are the amplitude, which is of course higher when more energy is pumped into

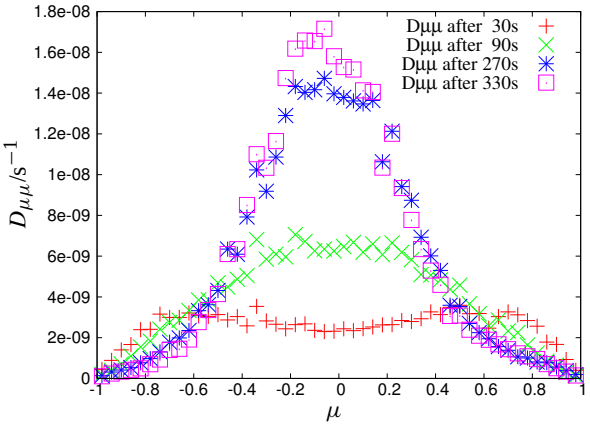

Fig. 11. Pitch angle diffusion coefficient for slow particles, incompressible driving, driving $k=1$

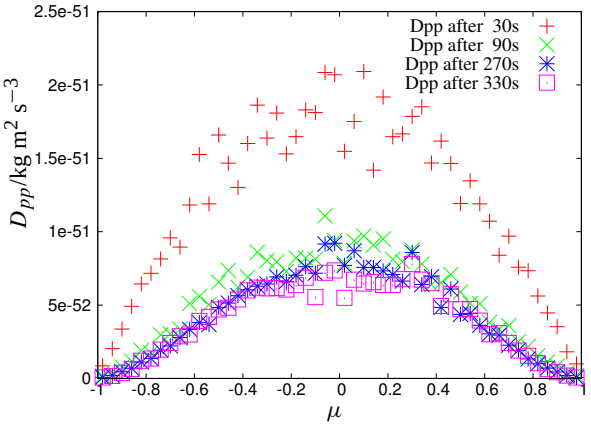

Fig. 13. Momentum diffusion coefficient for slow particles, compressible driving, driving $k=1$ and 2

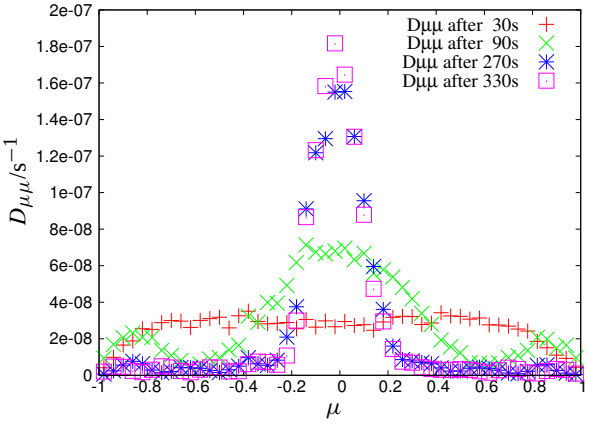

Fig. 12. Pitch angle diffusion coefficient for fast particles, incompressible driving, driving $k=1$

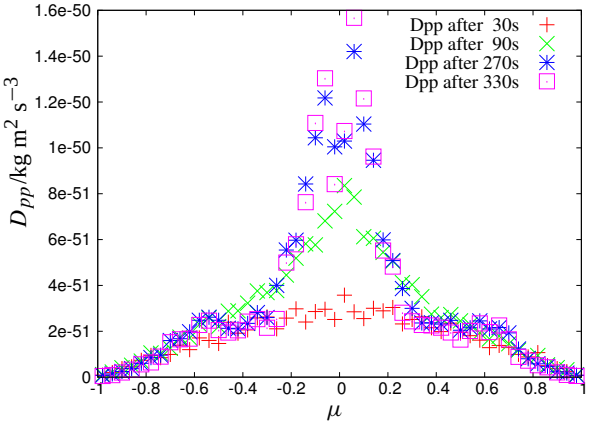

Fig. 14. Momentum diffusion coefficient for fast particles, compressible driving, driving $k=1$ and 2

the system (i.e. test case 2) also there the peak is broadened. For the fast particles not only the amplitude of the central peak is decreased in the fundamental wave case, but also the gyroresonance is almost vanished. This may be explained by the fact that the fast particles resonate closely to $k=2$. Additionally the resonance broadening, which is present in our thermal plasma, is less pronounced for faster particles.

4.3 Momentum diffusion

Additionally for higher order wave case the momentum diffusion coefficient D_{pp} has been calculated. Again compressible or incompressible modes have been used for driving for slow and fast particles. Results are shown in Figs. 13 – 16.

The comparison of momentum diffusion coefficients proves the result from the pitch angle diffusion coefficient: Slow particles show a strong scattering at $\mu=0$, which is approximately the same for compressible and incompressible driving. The fast particles show gyroresonances which are more pronounced in the incompressible driving case. The overall scattering is also stronger for fast particles, where the increase is in approximately given by Shalchi and Schlickeiser (2004, Eq. 85) for particle energies well below the rest energy.

5 Conclusions

We have shown simulations of the transport of charged particles in MHD plasmas without any assumptions on the underlying physics. Simple test cases have proven that our code is able to track particles, while extended test cases could give insight into wave-particle interaction in more complex situations. It should be however noted that this is not yet a fully evolved turbulent spectrum.

The main advantage of this method over previously used methods (Qin et al., 2006; Giacalone and Jokipii, 1999; Michałek and Ostrowsky, 1996; Tautz, 2010) is of course the

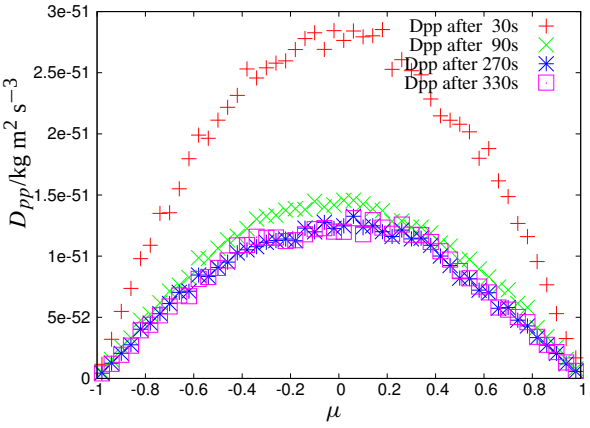

Fig. 15. Momentum diffusion coefficient for slow particles, incompressible driving, driving $k = 1$ and 2

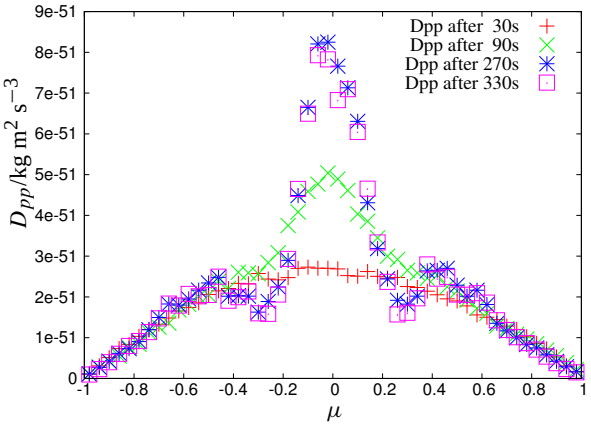

Fig. 16. Momentum diffusion coefficient for fast particles, incompressible driving, driving $k = 1$ and 2

spectrum put in. In our case only the outer parameters of turbulence (i.e. box size, boundary conditions, driving mechanism) are defined and all other processes are either the MHD evolution or particle motion by first principles. This in turn yields also the largest drawback: We are far more limited in the maximum extent of our turbulent spectrum. In our opinion the presented method is still a step ahead since it is no longer necessary to infer assumptions about correlations. A comparison of results like those of Qin and Shalchi (2009) seems difficult at this point, since in this test case an artificial spectrum is used.

What is different to standard QLT calculations is that here not single waves, but also subsequently produced waves are taken into account especially in electrodynamic (i.e. not magnetostatic) mode. In our results the influence of the wave electric field may be seen at $\mu = 0$ which produces a not expected perpendicular diffusion.

As an outlook it should be noted that this study can and will be used to study the interaction of charged particles with fully evolved turbulence to tackle the question of mean free path and angular distribution for example of solar energetic particles in the heliosphere. In a forthcoming paper a detailed study will be presented showing results for the mean free path in the solar wind. The applicability of this code is mainly limited by the applicability of the MHD description for the background plasma and the computer resources available. The major problem in this kind of simulation is that one either has to produce a turbulent spectrum for each particle energy or use box sizes of more than 1024^3 grid points.

Acknowledgements. FS acknowledges support by Deutsche Forschungsgemeinschaft through grant SP 1124-3, MW is supported by Graduiertenkolleg 1147.

Edited by: H. Fichtner
Reviewed by: two anonymous referees

References

Armstrong, J. W., Rickett, B. J., and Spangler, S. R.: Electron density power spectrum in the local interstellar medium, Astrophys. J., 443, 209–221, doi:10.1086/175515, 1995.

Balogh, A., Smith, E. J., Tsurutani, B. T., Southwood, D. J., Forsyth, R. J., and Horbury, T. S.: The Heliospheric Magnetic Field Over the South Polar Region of the Sun, Science, 268, 1007–1010, doi:10.1126/science.268.5213.1007, 1995.

de Avillez, M. A. and Breitschwerdt, D.: The Generation and Dissipation of Interstellar Turbulence: Results from Large-Scale High-Resolution Simulations, Astrophys. J. Lett., 665, L35–L38, doi:10.1086/521222, 2007.

Fichtner, H.: private communication, 2010.

Giacalone, J. and Jokipii, J. R.: The Transport of Cosmic Rays across a Turbulent Magnetic Field, Astrophys. J., 520, 204–214, doi:10.1086/307452, 1999.

Goldreich, P. and Sridhar, S.: Toward a theory of interstellar turbulence. 2: Strong alfvenic turbulence, Astrophys. J., 438, 763–775, doi:10.1086/175121, 1995.

Jokipii, J. R.: Cosmic-Ray Propagation. I. Charged Particles in a Random Magnetic Field, Astrophys. J., 146, 480, doi:10.1086/148912, 1966.

Kissmann, R. and Grauer, R.: A low dissipation essentially non-oscillatory central scheme, Computer Physics Communications, 176, 522–530, doi:10.1016/j.cpc.2006.11.014, 2007.

Kurganov, A. and Petrova, G.: A third-order semi-discrete central scheme for hyperbolic conservation laws and related problems, Numer. Math., 88, 683–729, 2001.

Maron, J. and Goldreich, P.: Simulations of Incompressible Magnetohydrodynamic Turbulence, Astrophys. J., 554, 1175–1196, doi:10.1086/321413, 2001.

Michałek, G. and Ostrowsky, M.: Cosmic ray momentum diffusion in the presence of nonlinear Alfvén waves, Nonlinear Processes in Geophysics, 3, 66–76, 1996.

Qin, G. and Shalchi, A.: Pitch-Angle Diffusion Coefficients of Charged Particles from Computer Simulations, Astrophys. J., 707, 61–66, doi:10.1088/0004-637X/707/1/61, 2009.

Qin, G., Matthaeus, W. H., and Bieber, J. W.: Parallel Diffusion of

Charged Particles in Strong Two-dimensional Turbulence, Astrophys. J. Lett., 640, L103–L106, doi:10.1086/503028, 2006.

Riquelme, M. A. and Spitkovsky, A.: Nonlinear Study of Bell's Cosmic Ray Current-Driven Instability, Astrophys. J., 694, 626–642, doi:10.1088/0004-637X/694/1/626, 2009.

Schlickeiser, R.: Cosmic-ray transport and acceleration. I - Derivation of the kinetic equation and application to cosmic rays in static cold media. II - Cosmic rays in moving cold media with application to diffusive shock wave acceleration, Astrophys. J., 336, 243–293, doi:10.1086/167009, 1989.

Shalchi, A.: Second-order quasilinear theory of cosmic ray transport, Physics of Plasmas, 12, 052 905, doi:10.1063/1.1895805, 2005.

Shalchi, A. and Schlickeiser, R.: Cosmic ray transport in anisotropic magnetohydrodynamic turbulence. III. Mixed magnetosonic and Alfvénic turbulence, Astron. Astrophys., 420, 799–808, doi:10.1051/0004-6361:20034304, 2004.

Shalchi, A., Bieber, J. W., and Matthaeus, W. H.: Nonlinear Guiding Center Theory of Perpendicular Diffusion in Dynamical Turbulence, Astrophys. J., 615, 805–812, doi:10.1086/424687, 2004.

Shalchi, A., Lazarian, A., and Schlickeiser, R.: Non-linear damping of slab modes and cosmic ray transport, Mon. Not. R. Astron. Soc., 383, 803–808, doi:10.1111/j.1365-2966.2007.12590.x, 2008.

Tautz, R. C.: A new simulation code for particle diffusion in anisotropic, large-scale and turbulent magnetic fields, Computer Physics Communications, 181, 71–77, doi:10.1016/j.cpc.2009.09.002, 2010.

Tautz, R. C., Shalchi, A., and Schlickeiser, R.: Solving the 90 degree Scattering Problem in Isotropic Turbulence, Astrophys. J. Lett., 685, L165–L168, doi:10.1086/592498, 2008.